Monthly Notices
of the
ROYAL ASTRONOMICAL SOCIETY

Mon. Not. R. Astron. Soc. **401,** 1375–1380 (2010) doi:10.1111/j.1365-2966.2009.15743.x

Multiple ionization sources in H II regions and their effect on derived nebular abundances

B. Ercolano,[1,2]★ R. Wesson[2] and N. Bastian[1]

[1]*Institute of Astronomy, Madingley Rd, Cambridge CB3 0HA*
[2]*Department of Physics and Astronomy, University College London, WC1E 6BT*

Accepted 2009 September 18. Received 2009 September 17; in original form 2009 September 3

ABSTRACT

We present a theoretical investigation of the effect of multiple ionization sources in H II regions on the total elemental abundances derived from the analysis of collisionally excited emission lines. We focus on empirical methods based on direct temperature measurements that are commonly employed in cases when the temperature of the nebular gas can be determined from the ratio of nebular to auroral lines of (e.g.) doubly ionized oxygen. We find that direct temperature methods that employ a two-temperature zone approach (DT2T methods) are very robust against the spatial distribution of sources. Errors smaller than 0.15 dex are estimated for regions where the metallicity is twice solar and errors below 0.05 dex for solar metallicities and below. The biases introduced by the spatial distribution of the ionization sources are thus much smaller for DT2T methods than for strong line methods, previously investigated by Ercolano, Bastian & Stasińska. Our findings are in agreement with the recent study of H II regions in NGC 300 by Bresolin et al.

Key words: ISM: abundances – H II regions – galaxies: abundances – galaxies: ISM.

1 INTRODUCTION

The analysis of emission lines from H II regions powered by OB stars is often the only means available for the determination of gas abundances both in our Galaxy and others. Accurate abundance determinations are crucial to derive metallicity gradients, which provide a key observational constraint to chemical evolution models of galaxies. The spectra of H II regions in the optical and infrared are dominated by collisionally excited lines (CELs) of singly and doubly ionized ions of some of the more abundant heavy elements (e.g. oxygen, carbon etc.). While the metallicity diagnostic power of CELs from H II regions is widely recognized and used for studying the chemical composition of galaxies, the uncertainties inherent to the empirical methods employed are often overlooked, potentially leading to somewhat over-optimistic error estimates.

Ionic abundances can be obtained from emission lines via the solution of the statistical equilibrium equation under the assumption of a gas temperature and density. Both gas temperature and density can be empirically derived from the observations using the ratio of diagnostic emission lines (e.g. Osterbrock & Ferland 2006). A widely used temperature diagnostic relies on the ratio of nebular to auroral [O III] lines, in particular ([O III]λ5007+[O III]λ4959)/[O III]λ4363. This method is often referred to as the 'direct temperature' method. For faint (distant) or metal-rich regions, however, the [O III]λ4363 line is seldom detected, rendering impossible the direct determination of temperature. In these cases, one is often forced to use 'strong-line methods', which rely on ratios of some of the strongest CELs calibrated with one-dimensional photoionization models. In a previous paper (Ercolano, Bastian & Stasińska 2007, hereafter EBS07), we showed that commonly employed strong-line methods may introduce a *systematic* bias of typically 0.1–0.3 dex, but up to 1 dex on the logarithmic oxygen abundance for regions where the gas and the ionising stars are intermixed.

Direct-temperature methods should be more reliable than strong line methods; however, even these are not entirely immune by errors introduced by calibrations from spherically symmetric models. While the error on the determination of a single ionic abundance from emission lines via the solution of the statistical equilibrium matrix is simply determined by the accuracy of the gas temperature and (to a lesser extent) density estimates, not all the ionic stages of a given element produce emission lines in the observed wavelength range. For this reason, the determination of total elemental abundances from ionic abundances relies on a correction for the unseen stages of ionization, known as the ionization correction factor (ICF). A potential bias is therefore introduced by the ICF schemes that are themselves calibrated via one-dimensional photoionization modelling (e.g. Kingsburgh & Barlow 1994, hereafter KB94; Peimbert, Torres-Peimbert & Ruiz 1992, hereafter PTR92), with the implied assumption of a geometry comprising of a spherical region with a single central location for all ionization sources.

The aim of this paper is to estimate whether the use of ICF schemes to derive total elemental abundances of H II regions from direct-temperature methods introduces a bias in the case of regions

★E-mail: be@ast.cam.ac.uk

ionized by multiple stars intermixed with the nebular gas. Via the analysis of theoretical H II region spectra obtained with the MOCASSIN code (Ercolano et al. 2003; Ercolano, Barlow & Storey 2005; Ercolano et al. 2008) in the set-up used by EBS07, we show that, unlike strong line methods, direct temperature methods using a two-temperature approach are very reliable also in cases when the stars are fully distributed within the nebular gas. These results are in line with the recent findings of Bresolin et al. (2009, hereafter B09) who found good agreement between CEL abundances obtained by direct temperature methods with the abundances derived from absorption line analysis of stellar photospheres in a sample of H II regions in the spiral galaxy NGC 300.

The paper is organized as follows. Section 2 summarizes the model set-up and input parameters. Section 3 contains a brief description of the methods employed. Our results are given in Section 4, while Section 5 is dedicated to a discussion and conclusions.

2 THEORETICAL EMISSION LINE SPECTRA: MODEL SET-UP AND INPUT PARAMETERS

We have used the theoretical nebular spectra of EBS07, which were obtained using the three-dimensional photoionization code MOCASSIN (Ercolano et al. 2003, 2005, 2008). This code uses a Monte Carlo approach to the transfer of radiation and can easily deal with multiple ionization sources arbitrarily distributed within the simulation region. The atomic data base included opacity data from Verner et al. (1993) and Verner & Yakovlev (1995), energy levels, collision strengths and transition probabilities from version 5.2 of the CHIANTI data base (Landi & Philips 2006, and references therein) and the improved hydrogen and helium free-bound continuous emission data of Ercolano & Storey (2006). The model set-up and input parameters are described in EBS07, here we summarize briefly the main points, but refer the interested reader to EBS07 for further details.

The regions are assumed to be spherical and consisting of homogeneous gas with number density $N_{\rm H} = 100$ cm^{-3}. The total number of ionising photons is constant for all models and is $Q_{\rm H^0} = 2.8 \times 10^{50}$ s^{-1}. We consider models of five different metallicities ($Z/Z_{\odot} = 0.05$, 0.2, 0.4, 1.0 and 2.0). The solar abundance model assumes the values of Grevesse & Sauval (1998) with the exception of C, N and O abundances which are taken from Allende Prieto, Lambert & Asplund (2002), Holweger (2001) and Allende Prieto, Lambert & Asplund (2001), respectively. The higher and lower metallicity cases were obtained from the solar abundances by scaling using the empirical abundance trends observed in H II regions by Izotov et al. (2006). The gas is ionized by 240 sources belonging to two populations, a hot ($M_* = 56\,{\rm M}_{\odot}$) and cool ($M_* = 37\,{\rm M}_{\odot}$) population, each population, as a whole, emits equal quantities of H-ionising photons. The stellar spectra were computed with the STARBURST99 spectral synthesis code (Leitherer et al. 1999) with the up-to-date non-LTE stellar atmospheres implemented by Smith, Norris & Crowther (2002) using single isochrones for the appropriate stellar masses. The stars were distributed as follows: (i) centrally concentrated at the centre of the spherical region – C-models; (ii) distributed in the half-volume of the spherical region – H-models and (iii) distributed in the full spherical volume – F-models. In the C-models, all stars share the same location at the origin of the Cartesian axes. In the H- and F-models, the stars are distributed stochastically such as to obtain a statistically homogeneous three-dimensional distribution of sources in the half or full spherical region, respectively. The Stroemgren sphere of stars in the F-models seldom overlap, while those of the C-model completely overlap, with the H-model representing the intermediate case.

In Table 1, we list the subset of the emission lines from our theoretical spectra that were used for the analysis described in the following section.

3 THE DIRECT TEMPERATURE METHOD

The aim of this study is to test whether the abundances determined from the emission line spectrum of an H II region ionized by multiple stars intermixed with the gas are different from the abundances determined by a region with exactly the same physical characteristics but with all ionization sources concentrated in the centre. EBS07 indeed demonstrated that large biases are introduced by this effect when strong-line methods are used. The main reason for such differences was due to a decrease of the 'effective ionization parameter' of the gas when the stars were fully distributed within the medium compared to when the same stars were all concentrated at the centre of the nebula. This affected the temperature structure of the nebula significantly enough to produce large errors in the derived abundances.

Ionic abundances from direct-temperature methods should be immune from this error as long as the temperature gradients within a given ionic phase are not too large (see e.g. Stasińska 1980; Kingdon & Ferland 1995). However, total elemental abundances can only be obtained by applying an ICF scheme to correct for the unseen ionization stages. The question therefore remains as to what is the effect of the geometrical distribution of the stars on the ICFs, which rely on theoretical calibrations via one-dimensional photoionization models (e.g. KB94; PTR92).

To answer this question, we took a subset of lines typically observed in extragalactic H II regions, including the important temperature diagnostic lines of [O III] at 4363 Å and [N II] at 5754 Å, from the line spectra produced by the photoionization models described in Section 2. We then used these model spectra to derive chemical abundances via the direct temperature method. The lines used for the analysis are listed in Table 1.

We considered the nebula as being composed of two separate zones of low and high ionization: first, we assumed a temperature of 10 000 K to obtain electron densities from the [O II] λ3726/λ3729 and [S II] λ6717/λ6731 line ratios. Then, the average of these two electron densities was used to derive a temperature from the [N II] (λ6548+6584)/λ5754 line ratio. This temperature was then used to recalculate the densities, and the temperature recalculated once more using the resulting density. The abundances of singly ionized species were derived using this temperature and density. Then, we used the same iterative approach, but using the [Cl III] 5517/5537 and [Ar IV] 4711/4740 line ratios as density diagnostics, and the [O III] 4959+5007/4363 ratio as a temperature diagnostic. Abundances of doubly and more highly ionized species were derived using this temperature and density.

Total abundances relative to hydrogen were calculated for He, C, N, O, Ne, S and Ar, using the two commonly used ICF schemes of KB94 and PTR92. For several atoms these schemes use the same correction; they differ for helium (KB94 do not correct for neutral helium while PTR92 does), argon and sulphur.

We also considered the case where a low-ionization temperature diagnostic is not available. In this situation, one can either use the [O III] temperature for all ions or estimate the low ionization temperature using relations such as that found by Pilyugin, Vílchez & Thuan (2006). We confirm previous findings that applying a single temperature diagnostics introduces considerable errors

Table 1. Model emission line fluxes, relative to Hβ = 100.

λ (Å)	Ion	Model														
		0.05c	0.05f	0.05h	0.20c	0.20f	0.20h	0.40c	0.40f	0.40h	1.00c	1.00f	1.00h	2.00c	2.00f	2.00h
3726.03	[O II]	12.38	27.70	14.07	40.05	87.69	35.55	35.20	95.33	32.05	18.55	48.28	17.57	63.89	62.60	55.92
3728.82	[O II]	16.51	37.10	18.78	53.18	116.7	47.19	46.62	126.5	42.47	24.34	63.43	23.04	82.17	80.68	71.92
3868.75	[Ne II]	22.93	11.58	21.12	43.07	26.43	44.01	31.03	21.10	31.42	2.682	2.433	2.410	0.034	0.149	0.040
3967.46	[Ne II]	6.910	3.491	6.363	12.97	7.965	13.25	9.349	6.359	9.468	0.808	0.733	0.726	0.010	0.045	0.012
4068.60	[S II]	0.471	1.828	0.634	1.426	5.011	1.341	1.590	6.435	1.547	1.020	4.000	0.950	0.351	1.072	0.331
4076.35	[S II]	0.163	0.632	0.219	0.493	1.734	0.464	0.550	2.227	0.535	0.354	1.390	0.329	0.122	0.374	0.115
4363.21	[O III]	9.693	3.995	8.741	8.649	4.593	9.138	2.993	1.747	3.037	0.070	0.045	0.053	0.002	0.005	0.002
4471.50	He I	4.150	4.186	4.143	4.328	4.241	4.305	4.469	4.295	4.460	4.723	4.476	4.723	4.293	4.356	4.345
4685.68	He II	0.008	0.011	0.010	0.013	0.013	0.013	0.007	0.010	0.009	0.006	0.009	0.006	0.003	0.001	0.002
4711.37	[Ar IV]	1.385	0.491	1.235	2.319	0.898	2.451	1.765	0.710	1.890	0.081	0.047	0.082	0.000	0.002	0.001
4740.17	[Ar IV]	1.069	0.377	0.952	1.737	0.672	1.838	1.295	0.520	1.386	0.059	0.034	0.060	0.000	0.001	0.000
4861.33	H I	100.0	100.0	100.0	100.0	100.0	100.0	100.0	100.0	100.0	100.0	100.0	100.0	100.0	100.0	100.0
4958.91	[O III]	110.1	52.62	101.5	200.4	116.4	207.7	161.3	102.3	165.2	19.47	16.55	17.97	1.854	4.190	1.844
5006.84	[O III]	328.6	157.0	303.0	598.0	347.4	619.8	481.5	305.2	493.0	58.11	49.40	53.64	5.531	12.50	5.504
5754.60	[N II]	0.026	0.059	0.030	0.076	0.165	0.068	0.097	0.258	0.089	0.075	0.193	0.071	0.237	0.266	0.215
5875.66	He I	10.87	11.16	10.87	11.57	11.42	11.50	12.27	11.80	12.23	14.32	13.22	14.26	14.12	13.42	14.15
6312.10	[S III]	0.923	1.045	0.982	2.261	2.867	2.142	1.868	2.573	1.686	0.458	0.743	0.410	0.368	0.309	0.320
6548.10	[N II]	0.321	0.943	0.396	1.114	2.919	1.017	1.895	5.979	1.784	2.831	9.155	2.741	16.14	21.44	15.15
6562.77	H I	276.8	280.8	277.3	281.2	283.0	281.1	286.8	287.1	286.7	306.5	301.3	305.7	314.4	306.6	313.7
6583.50	[N II]	0.981	2.880	1.209	3.402	8.916	3.107	5.787	18.26	5.449	8.647	27.96	8.371	49.31	65.50	46.28
6678.16	He I	2.983	3.115	2.993	3.238	3.214	3.218	3.486	3.354	3.476	4.080	3.784	4.069	3.864	3.792	3.905
6716.44	[S II]	4.194	17.80	5.839	12.84	50.82	12.43	16.03	70.59	15.77	13.80	61.42	13.08	6.061	21.11	5.783
6730.82	[S II]	3.100	13.11	4.314	9.524	37.39	9.199	11.83	51.96	11.64	10.15	45.06	9.619	4.447	15.50	4.242
7136.80	[Ar III]	0.808	1.193	0.875	2.969	4.414	2.833	3.662	5.865	3.412	2.342	4.033	2.205	3.014	4.011	2.592
7319	[O II]	0.544	1.025	0.597	1.479	2.856	1.290	1.015	2.393	0.902	0.311	0.676	0.291	0.644	0.568	0.551
7330	[O II]	0.443	0.836	0.487	1.205	2.329	1.052	0.828	1.953	0.736	0.254	0.552	0.238	0.526	0.464	0.450
7751.43	[Ar III]	0.194	0.286	0.210	0.711	1.058	0.679	0.877	1.405	0.818	0.561	0.966	0.528	0.722	0.961	0.621

into the abundance determinations. This case will not be further discussed.

4 RESULTS

Our analysis indicates that the errors on the abundances introduced by the geometrical distribution of the ionising stars are much smaller when direct temperature methods are used instead of strong line methods. We stress here that our aim is not to assess the validity of the ICFs but to assess the effect of the distribution of the ionising sources on the derived abundances. Therefore, we are not comparing the derived abundances to the 'right answer' (i.e. the input abundances for our models), but rather comparing the results from model nebulae with distributed ionising sources to those with a centrally concentrated source.

Fig. 1 shows the logarithmic error, E_{F-C}, on the abundances of various elements due to the spatial distribution of the ionization sources. The black solid line shows results using KB94 ICFs and the red dashed lines show the results for the ICF scheme of PTR92. The errors are due partly to temperature effects (e.g. a steep temperature profile or differences in the mean temperatures of various ions) and partly to the ICFs which may be more or less sensitive to changes in the effective ionization parameter brought about by a different spatial distribution of sources (see discussion in EBS07). Here, we are mostly interested in the latter, and in order to isolate this effect we calculate a correction to the error due to the ICFs, $\Delta(E_{F-C})$, by comparing the C and F-model theoretical and empirical ICFs

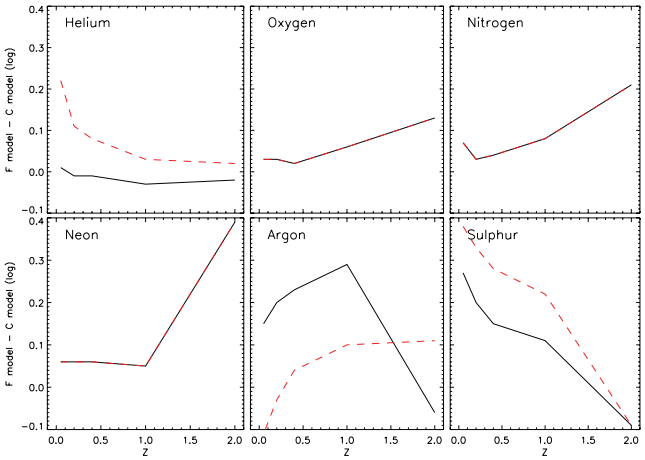

Figure 1. Error on the logarithmic abundances calculated via the DT2T method caused by the spatial distribution of ionization sources. The black solid line shows results obtained via the KB94 ICFs, while the red dashed line shows those obtained via the PTR92 ICFs.

according to the following:

$$\Delta(E_{F-C}) = \log_{10}\left(\frac{ICF_F^O}{ICF_C^O} \Big/ \frac{ICF_F^T}{ICF_C^T}\right), \quad (1)$$

where ICF_F^O, ICF_C^O are the observational ICFs for the F- and C-models, respectively, and ICF_F^T, ICF_C^T are their theoretical counterparts calculated by the photoionization model.

Table 2. Logarithmic errors and ICF corrections.

	Helium					Oxygen					Nitrogen			
$Z/Z_\odot$	E_{F-C}		$\Delta(E_{F-C})$		$Z/Z_\odot$	E_{F-C}		$\Delta(E_{F-C})$		$Z/Z_\odot$	E_{F-C}		$\Delta(E_{F-C})$	
	KB94	PTR92	KB94	PTR92		KB94	PTR92	KB94	PTR92		KB94	PTR92	KB94	PTR92
0.05	0.01	0.22	1.0	−0.14	0.05	0.03	0.03	1.0	1.0	0.05	0.07	0.07	−0.03	−0.03
0.2	−0.01	0.11	1.0	−0.06	0.2	0.03	0.03	1.0	1.0	0.2	0.03	0.03	+0.08	+0.08
0.4	−0.01	0.08	1.0	−0.03	0.4	0.02	0.02	1.0	1.0	0.4	0.04	0.04	+0.03	+0.03
1.0	−0.03	0.03	1.0	−0.007	1.0	0.06	0.06	1.0	1.0	1.0	0.08	0.08	−0.03	−0.03
2.0	−0.02	0.02	1.0	−0.047	2.0	0.13	0.13	1.0	1.0	2.0	0.21	0.21	−0.14	−0.14
	Neon					Argon					Sulphur			
$Z/Z_\odot$	E_{F-C}		$\Delta(E_{F-C})$		$Z/Z_\odot$	E_{F-C}		$\Delta(E_{F-C})$		$Z/Z_\odot$	E_{F-C}		$\Delta(E_{F-C})$	
	KB94	PTR92	KB94	PTR92		KB94	PTR92	KB94	PTR92		KB94	PTR92	KB94	PTR92
0.05	0.06	0.06	−0.07	−0.07	0.05	0.15	−0.11	−0.07	1.0	0.05	0.27	0.38	−0.21	−0.33
0.2	0.06	0.06	−0.04	−0.04	0.2	0.20	−0.03	−0.04	1.0	0.2	0.20	0.33	−0.16	−0.28
0.4	0.06	0.06	−0.006	−0.006	0.4	0.23	0.04	−0.004	1.0	0.4	0.15	0.28	−0.15	−0.27
1.0	0.05	0.05	+0.10	+0.10	1.0	0.29	0.10	−0.08	1.0	1.0	0.11	0.22	−0.9	−0.18
2.0	0.39	0.39	+0.41	+0.41	2.0	−0.06	0.11	+0.16	1.0	2.0	−0.090	−0.09	−0.023	−0.02

The logarithmic errors and the ICF corrections are summarized in Table 2. In the following, we will discuss the sources of error in more detail for each element.

4.1 Helium

KB94 do not include an ICF correction for the unseen neutral helium; the very small E_{F-C} for KB94 shown in Fig. 1 is therefore only due to the lack of correction and the C- and F-models having different amounts of neutral helium. PTR92 on the other hand correct for neutral helium and it is indeed the ICF correction employed that at low metallicities is sensitive to changes in the effective ionization parameter. The $\Delta(E_{F-C})$ corrections given in Table 2 drastically reduce the E_{F-C} values for PTR92.

4.2 Oxygen

The abundance of oxygen derived by the direct temperature method with a two temperature description of the medium (DT2T) is not very sensitive to the geometrical distribution of the ionization sources (i.e. to the effective ionization parameter) for the range of metallicities discussed here. The largest errors occur for metal-rich regions (twice solar) and are always below 0.15 dex. We note that both the empirical and theoretical ICFs for oxygen are roughly unity for all models considered here. The small error at higher metallicities is due to the steepening of the temperature profile which is more accentuated for the C-models (see discussion in EBS07 and Stasińska 1980). This causes the oxygen abundances to be underestimated in the C-models more than in the F-models producing the error observed.

4.3 Nitrogen

Nitrogen also shows a similar behaviour with a slightly larger error (0.21 dex) for metal-rich regions. The nitrogen ICFs are not unity and some of the error shown in Fig. 1 are indeed due to a different response of the ICFs to the change in the effective ionization potential. The ICF correction is $\Delta(E_{F-C}) = -0.14$ for nitrogen in the $Z/Z_\odot = 2$ case, which brings the nitrogen E_{F-C} to roughly 0.1 dex. The remainder of the error can again be ascribed to the steepening of the temperature profile as discussed above.

4.4 Neon

The situation for neon is more complicated. $\Delta(E_{F-C})$ at $Z/Z_\odot = 2$ is $\sim +0.3$ dex, which actually increases the magnitude of the error. The large discrepancy ($E_{F-C} \sim 0.7$!) is due to the displacement of the Ne^{2+} and O^{2+} regions which results in a significant difference between $T_e(Ne^{2+})$ and $T_e(O^{2+})$ at high Z's. Using $T_e(O^{2+})$ in the determination of Ne^{2+} abundance then results in the large error. Indeed, we find that at $Z/Z_\odot = 2$, $T_e(Ne^{2+})/T_e(O^{2+}) = 0.85$ for the C-model and 0.93 for the F-model, the difference has a significant impact on abundances derived via CELs due to their exponential dependence on temperature. We calculate the correction due to the difference in the two temperature regions to be −0.61 dex, which brings the total E_{F-C} to roughly 0.1 dex, which is comparable to what we found for oxygen and nitrogen.

4.5 Argon

PTR92 do not employ a correction for Ar^+, and the small errors shown are due to the change in the ionization structure of F- and C-models. KB94 do include an ICF for Ar, however this is quite sensitive to changes to the effective ionization parameter. The maximum errors for KB94 are of 0.3 dex at solar metallicities against a maximum error of 0.1 dex obtained by PTR92 at $Z/Z_\odot = 0.05$.

4.6 Sulphur

Sulphur presents larger problems at low metallicities for both methods with maximum errors of 0.4 dex at $Z/Z_\odot = 0.05$ for PTR92 and 0.27 dex for KB94 at the same metallicity. Most of the error here can be ascribed to the different responses of the ICFs to the change of the effective ionization parameter. Indeed, applying the $\Delta(E_{F-C})$ corrections given in Table 2 brings E_{F-C} to values smaller than 0.1 dex both for KB94 and PTR92.

The results obtained for the H-models lie in between those of the F and C models and are therefore not included in this discussion.

5 DISCUSSION AND CONCLUSIONS

The main conclusion of this short paper is that abundance determinations from collisionally excited emission lines (CELs) of H II

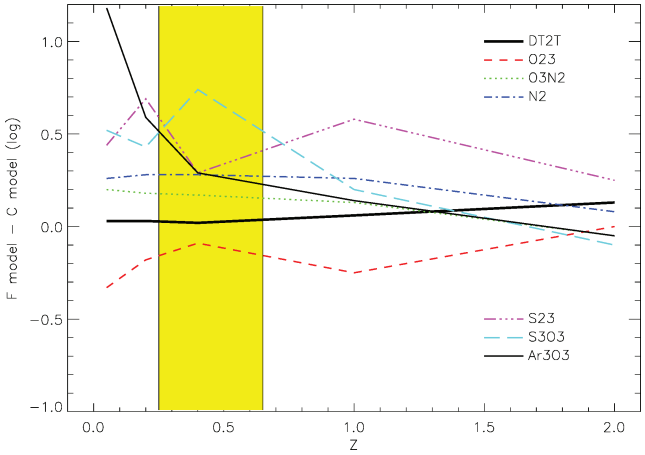

Figure 2. Errors on the logarithmic abundances calculated via the DT2T method caused by the spatial distribution of ionization sources. The black solid line shows results obtained via the DT2T method. The thinner lines show results obtained from strong line methods, namely as follows. Red dashed: O23 (Pilyugin 2000, 2001); green dotted: O3N2 (Stasińska 2006); blue dash dotted: N2 (PP04); magenta dash double dot: S23 (Pérez-Montero & Diaz 2005); cyan long dash: S3O3 (Stasińska 2006); black thin solid: Ar3O3 (Stasińska 2006). The yellow shaded region indicates the metallicity range of the H II regions in NGC 300 analysed by B09.

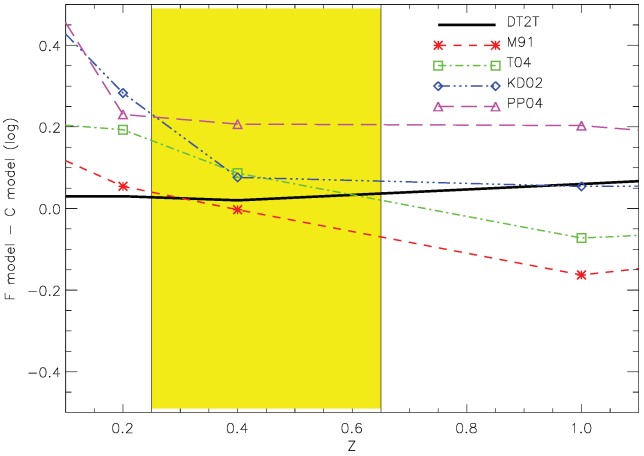

Figure 3. Errors on the logarithmic abundances calculated via the DT2T method caused by the spatial distribution of ionization sources. The black solid line shows results obtained via the DT2T method. The thinner lines show results obtained from the strong line methods analysed by B09. See text for details.

regions via direct temperature methods that use a two-temperature description of the ionized region are very robust and not affected significantly by the spatial distribution of ionization sources. Indeed, the maximum errors on the oxygen abundance derived with the DT2T method are still lower than 0.15 dex at $Z = 2$ and below 0.05 dex at solar metallicity and below.

As a comparison we found that the strong-line-methods analysed in EBS07 gave much larger errors as shown in Fig. 2. The figure shows the discrepancy in the empirically determined oxygen abundance for the F- (fully distributed) and C- (centrally concentrated) models. The thick black line indicates the results for the DT2T, while the thinner lines are for the results of the various strong line methods considered by EBS07. A detailed legend is provided in the caption to Fig. 2. The small errors associated with the DT2T method compared to the large errors of the strong line methods are in agreement with the recent results of B09 who found a systematic difference between the oxygen abundance calculated by strong line methods and direct temperature methods for a sample of H II regions in NGC 300. The yellow section in Fig. 2 shows the metallicity range of the H II regions analysed by B09. B09 compared the metallicities obtained by a direct temperature and a strong-line analysis of the emission line spectra of H II regions in NGC 300 to those obtained from B and A supergiants in the same galaxy. They found excellent agreement between the results from supergiants and direct temperature analysis of the H II regions, while noting that a systematic bias affected the results from some popular calibration of strong lines. The calibrations used in B09 were not considered by EBS07 and included (i) the R23[1] ratio from the theoretical calibration of McGaugh (1991, hereafter M91) using the analytical prescriptions of Kuzio de Naray et al. (2004) and Tremonti et al. (2004, hereafter T04, their equation 1), (ii) the theoretical prediction for the [N II]λ6583/[O II]λ3727 ratio by Kewley & Dopita (2002, hereafter KD02) and (iii) N2 = log([N II]λ6583/Hα), calibrated empirically by Pettini & Pagel (2004, hereafter PP04).

In order to estimate whether the spatial distribution of stars may be playing a role in producing the bias observed by B09 and predicted by EBS07, we have used the emission line spectra in Table 1 to compute the oxygen abundances given by the M91, T04, KD02 and PP04 calibrations listed above and compared it to the DT2T results in Fig. 3. The metallicity range of the B09 sample is again highlighted by the yellow section. The errors of the strong line methods are comparable to those lamented in the B09 paper, however a detailed comparison with the observation is premature at this point. The main problem is that the set of models run by EBS07 comprised a very idealised ionising source population which was designed to highlight eventual temperature fluctuations that may be introduced by the distribution of stars with spectra of very different hardness (see also Section 2), which turns out to be equivalent to a much harder 'effective' spectrum than that inferred by B09 for the H II regions in NGC 300. The parameter $\eta = (O^+/O^{++})/(S^+/S^{++})$, (Vilchez & Pagel 1988) was introduced as a measure of the hardness of the ionising field, with larger numbers corresponding to a softer spectrum. B09 find an average log(η) parameter of roughly 0.7, while we find values ranging between −0.2 and 0.2, indicating a significantly harder spectrum than that of the B09 H II regions. Another problem is the fact that EBS07 explored a wide metallicity range and as a consequence the narrow metallicity range of the H II regions in NGC 300 is very sparsely sampled, as shown in Fig. 3 only one model data point actually falls in that range. In view of these shortcomings of the models we can at present only suggest that the spatial distribution of ionising sources is the cause of the metallicity bias that afflicts strong line measurements and postpone firmer statements to a future work where the parameter range is better suited to match those particular observations.

We finally note that we have not included a discussion of the well-known abundance discrepancy between CELs and recombination lines. A number of possible causes have been identified in the literature including temperature fluctuations (Peimbert 1967), hydrogen-deficient, metal-rich inclusions (Liu et al. 2000; Stasińska et al. 2007) and X-ray irradiated quasi-neutral clumps (Ercolano 2009). The jury is still out however as to which of the above effects

[1] R23 = ([O II]λ3727 + [O III]λ37274959,5007)/Hβ.

or a combination thereof is to blame for the discrepancy. Until the latter problem is resolved all abundances determined via nebular emission lines carry a potential error. The excellent agreement between the results obtained by B09 from direct temperature analysis of CELs and those from the supergiants in NGC 300, however, indicates that in this Galaxy temperature fluctuations and X-ray irradiated quasineutral clumps, if at all present, must be playing a minor role.

ACKNOWLEDGMENTS

BE and NB are supported by a Science and Technology Facility Council Advanced Fellowship.

REFERENCES

Allende Prieto C., Lambert D. L., Asplund M., 2001, ApJ, 556, L63
Allende Prieto C., Lambert D. L., Asplund M., 2002, ApJ, 573, L137
Bresolin F., Gieren W., Kudritzki R.-P., Pietrzyński G., Urbaneja M. A., Carraro G., 2009, ApJ, 700, 309 (B09)
Ercolano B., 2009, MNRAS, 397, L69
Ercolano B., Storey P. J., 2006, MNRAS, 372, 1875
Ercolano B., Barlow M. J., Storey P. J., Liu X.-W., 2003, MNRAS, 340, 1136
Ercolano B., Barlow M. J., Storey P. J., 2005, MNRAS, 362, 1038
Ercolano B., Bastian N., Stasińska G., 2007, MNRAS, 379, 945 (EBS07)
Ercolano B., Young P. R., Drake J. J., Raymond J. C., 2008, ApJS, 175, 534
Grevesse N., Sauval A. J., 1998, Space Sci. Rev., 85, 161
Holweger H., 2001, Joint SOHO/ACE Workshop Solar and Galactic Composition, 598, 23
Izotov Y. I., Stasińska G., Meynet G., Guseva N. G., Thuan T. X., 2006, A&A, 448, 955
Kewley L. J., Dopita M. A., 2002, ApJS, 142, 35 (KD02)
Kingdon J., Ferland G. J., 1995, ApJ, 442, 714
Kingsburgh R. L., Barlow M. J., 1994, MNRAS, 271, 257 (KB94)
Kuzio de Naray R., McGraugh S. S., de Blok W. J. G., 2004, MNRAS, 355, 887
Landi E., Phillips K. J. H., 2006, ApJS, 166, 421
Leitherer C. et al., 1999, ApJS, 123, 3
Liu X.-W., Storey P. J., Barlow M. J., Danziger I. J., Cohen M., Bryce M., 2000, MNRAS, 312, 585
McGaugh S. S., 1991, ApJ, 380, 140 (M91)
Osterbrock D. E., Ferland G. J., 2006, Astrophysics of Gaseous Nebulae and Active Galactic Nuclei, 2nd. University Science Books, Sausalito, CA
Peimbert M., 1967, ApJ, 150, 825
Peimbert M., Torres-Peimbert S., Ruiz M. T., 1992, Rev. Mex. Astron. Astrofis., 24, 155 (PTR92)
Pettini M., Pagel B. E. J., 2004, MNRAS, 348, L59 (PP04)
Pérez-Montero E., Diaz A. I., 2005, MNRAS, 361, 1063
Pilyugin L. S., 2000, A&A, 362, 325
Pilyugin L. S., 2001, A&A, 369, 594
Pilyugin L. S., Vílchez J. M., Thuan T. X., 2006, MNRAS, 370, 1928
Smith L. J., Norris R. P. F., Crowther P. A., 2002, MNRAS, 337, 1309
Stasińska G., 1980, A&A, 85, 359
Stasińska G., 2006, A&A, 454, L127
Stasińska G., Tenorio-Tagle G., Rodríguez M., Henney W. J., 2007, A&A, 471, 193
Tremonti C. A. et al., 2004, ApJ, 613, 898 (T04)
Verner D. A., Yakovlev D. G., 1995, A&AS, 109, 125
Verner D. A., Yakovlev D. G., Band I. M., Trzhaskovskaya M. B., 1993, At. Data Nucl. Data Tables, 55, 233
Vilchez J. M., Pagel B. E. J., 1988, MNRAS, 231, 257

This paper has been typeset from a TEX/LATEX file prepared by the author.